CRISPR-Cas9 gene insertion in *Epichloë* species

Taryn A. MILLER[1], Debbie A. HUDSON[1], Nazanin NOORIFAR[2], Wade J. MACE[1], Richard D. JOHNSON[1] and Linda J. JOHNSON[1]*

[1]*AgResearch Group – Bioeconomy Science Institute, Grasslands Research Centre, Palmerston North, New Zealand*

[2]*Plant Health Laboratory, AsureQuality Ltd., Lincoln, New Zealand*

*Corresponding author: linda.johnson@agresearch.co.nz

Abstract

The dairy, meat, and fibre industries in several regions within New Zealand are heavily reliant on selected strains of endophytic fungi, within the genus *Epichloë*, which confer resistance to a range of insect pests and environmental pressures when in symbiosis with pasture cultivars. Unfortunately, some fungal strains are historically intractable to genetic manipulation, therefore preventing investigation into novel traits. Only recently with the development of CRISPR-Cas systems, a revolutionary gene editing tool, was CRISPR-Cas9 successfully used on one of these intractable strains, *Epichloë* sp. LpTG-3 strain AR37, to create targeted gene disruptions. This study focused on CRISPR-Cas9 targeted gene insertion capabilities in *Epichloë* spp. CRISPR-Cas9 was successfully deployed to precisely insert 236 bp of coding sequence from a critical condensation domain of the *perA* gene, missing in the genetically intractable *Epichloë festucae* var. *lolii* strain AR48. CRISPR-Cas9 was also successfully deployed to insert the reporter gene *gfp* into a precise location within the indole diterpene pathway, a known secondary metabolite pathway in AR37. This research illustrated the ability of CRISPR-Cas9 to repair or insert genes in genetically intractable *Epichloë* species, with the potential for reconstruction of secondary metabolite pathways for novel compound production and delivery into New Zealand's pasture-based agricultural system.

Keywords: genetic modification, GFP, indole diterpene, peramine, secondary metabolite

Introduction

Epichloë spp. are filamentous fungi that form symbiotic associations with Pooideae grasses. The grass provides nutrients to the fungus while the fungus protects the plant against herbivory through the production of insect and mammalian bioprotective secondary metabolites (Schardl 1996). Currently, there are four secondary metabolite pathways linked to compounds with demonstrated bioactivity: peramine (insect bioactive) (Tanaka et al. 2005), indole diterpenes (insect and mammalian bioactives) (Young et al. 2009), ergot alkaloids (insect and mammalian bioactives) (Panaccione et al. 2001), and lolines (insect bioactives) (Spiering et al. 2005). Natural fungal variants have been identified through genetic analysis for the presence, absence, and functionality of genes and is supported by chemical analysis of pathway intermediates and end compounds (Johnson et al. 2013; Schardl et al. 2013). This has led to subsequent commercialisation of grass seeds containing selected *Epichloë* strains to enhance pasture persistence and improve animal health and welfare *e.g.,* AR1, AR37, NEA-2, MaxP, and MaxQ. In New Zealand, *Epichloë* products contribute >NZ$200 million annually to the economy, with AR37 contributing NZ$3.6 billion over the lifetime of its patent (Caradus & Johnson 2019; Johnson & Caradus 2019).

Historically, *Epichloë* spp. have been genetically modified using protoplast mediated transformation in conjunction with either targeted homologous recombination or random integration. This genetic modification technique has been successfully utilised in some strains such as *Epichloë festucae* Fl1 to investigate the symbiotic interaction and secondary metabolite production through gene insertions and deletions (reviewed in Johnson et al. 2021). However, for other agriculturally important strains, such as AR37, these techniques have been less effective making genetic modification challenging.

CRISPR-Cas (Clustered Regularly Interspaced Short Palindromic Repeats/CRISPR Associated Protein) was discovered in bacteria and archaea as a primitive adaptive immune system and has now been utilised as a genetic modification tool that was awarded a Nobel Prize in Chemistry in 2020 (Uyhazi & Bennett 2021). The Cas9 protein creates a double stranded DNA

ISSN 2463-2872 (Print) ISSN 2463-2880 (Online) https://doi.org/10.33584/rps.18.2025.3763

break at a specific Protospacer Adjacent Motif (PAM) site identified by a specific guide RNA, which then induces the cells own DNA repair machinery through non-homologous end joining (NHEJ), microhomology-mediated end joining (MMEJ) or homologous repair (HR). This can result in deletion or insertion of DNA ranging from a single base indel/SNP to around 10 kb insertion (Zhang et al. 2015; Chu et al. 2016; Kato et al. 2017). This system has now been successfully used in a range of hosts (mammals, plants, insects, bacteria, and fungi) (Tong et al. 2018; Hendriks et al. 2020; Liu et al. 2020; Menchaca et al. 2020; Moradpour & Abdulah 2020; Jiang et al. 2021).

Over the last few years, the genetic modification of *Epichloë* using CRISPR-Cas9 has been successfully used to delete or inactivate genes for functional characterisation of secondary metabolite pathways, including gene inactivation of the epoxyjanthitrem pathway in AR37 and gene cluster deletion of the ergot alkaloid pathway in both *Epichloë coenophiala* strain e19 and *Epichloë hybrida* strain Lp1 (Wang et al. 2018; Florea et al. 2021; Miller et al. 2022). The next stage is the application of CRISPR-Cas9 for genetic insertion to either restore non-functional genes or add gene/s.

This paper demonstrates for the first time the repair of the *perA* gene through exon targeted CRISPR-Cas9 insertion. Peramine is a pyrrolopyrazine-containing secondary metabolite produced from a single non-ribosomal peptide synthetase (NRPS) enzyme encoded by a gene of approximately 8 kb in size called *perA*. The domain configuration of *perA* is adenylation 1, thioester 1, condensation, adenylation 2, methylation, thioester 2, and reductase (Berry et al. 2015). Peramine confers bioprotection against Argentine stem weevil, a major agricultural pest of perennial ryegrass pastures in New Zealand (Rowan et al. 1990). In the *E. festucae* var. *lolii* strain AR48, there is a 236 bp deletion in the condensation domain of *perA* (Miller 2018), making it an ideal first candidate for functional insertion repair *i.e.,* in contrast to inserting multiple kilobases for the whole gene. This was successfully achieved using template mediated CRISPR-Cas9 assisted targeted homologous recombination. The other target of this paper was successfully inserting the full-length reporter gene *gfp,* which encodes the green fluorescent protein (GFP), into the intergenic region of the indole diterpene pathway (IDT) in AR37 which was targeted using CRISPR-Cas9 assisted homologous recombination. This target was chosen as the next step for assessing insertion size *e.g.,* a single gene with promoter and terminator, as well as using the fluorescence characteristic for easy detection of gene insertion and expression.

In summary, the research described in this paper illustrates the ability of CRISPR-Cas9 to precisely insert genetic material into genetically intractable *Epichloë* spp. This opens the potential for reconstruction of secondary metabolite pathways for novel compound production and delivery into New Zealand's pasture-based agricultural system.

Materials and Methods

CRISPR-Cas9 Design and Assembly

Gene editing was performed using a CRISPR-Cas9 approach as described by Miller et al. (2022). The guides and transformation parameters used in this study are listed in Table 1. The template used for the *perA* repair was an amplicon from AR1 (Genebank KP834531.1). The template used for the *gfp* insertion was the 5' border (Genebank ON500678.1 – 58633 to 58434), the 3' border (Genebank ON500678.1 – 58972 to 58773) from AR37 genomic DNA and the Tef promoter (Genebank MH220818.1– 411 to 1200), the *gfp* gene (Genebank MF169984.1 – 1146 to 1865), the Tgla terminator (Genebank MF169984.1 – 1866 to 2068) from *gfp* plasmid and the kit plasmid backbone assembled using golden gate according to the manufacturer's instructions (New England Biolabs Inc., USA) (Table 2).

Microscopy imaging of GFP transformants

Sub-cultured CRISPR GFP transformants were assessed for fluorescence using a BX63 automated fluorescence microscope with a BX3 fluorescence mirror unit holding a U-FGFP cube and DP74 camera, analysed using cellSens V3.1 (Dimension software, Olympus Corp., Japan). The fluorescence status of each transformant was then assessed using the fluorescent microscope using multichannel or brightfield (710 µs exposure) and eGFP images (400 µs exposure) at 2× magnification, with image stitched used on whole plate images.

qPCR of *gfp* transformants

Copy number was assessed using a genome sequence confirmed single *gfp* inserted Fl1 strain (*gfp* primer = TCTTCTTCAAGGACGACGGC / CCTTGATG-CCGTTCTTCTGC) and native single copy NRPS (NRPS primers = GTCCGATCATTCCAAGCTCGTT/ TGGTGGGAAGTTCCCTGCAC) standard curves (11 ng/µL stock with 7 × 5-fold dilutions) on a LightCycler® 480 Instrument II (F. Hoffmann-La Roche AG, Switzerland) using a SYBR green kit (KAPA Biosystems Inc., USA) according to the manufacturer's instructions.

Table 1 Guide and transformation parameters.

Target	Strain	Guide name	Doench score	Insertion type	Insertion size (bp)	Border (bp)	Guide (fmol)	Template (fmol)
perA	AR48	434	0.487	Repair	236	~ 150 ~ 500	300	200
perA	AR48	912	0.569	Repair	236	~ 150 ~ 500	300	200
IDT	FI1/AR37	TM07	0.748	Gene	724	~200	600	60
IDT	FI1	TM08	0.493	Gene	724	~200	600	60
IDT	FI1	TM09	0.663	Gene	724	~200	600	60

Table 2 Primers used in this study.

Primer	AR48 peramine repair	AR37 GFP insertion
Guide	434: GAGGATTGCATCCCGGGCAGAGG 912: TCTGTTCCAAGTCCTCTGCCCGG	TM07: ACCTGCAGTAGTGGTCACCGTGG TM08: CCGTGGCTTTAAAAAGCTTTAAG TM09: CCGATGCATATTCTATGCAAAGT
5' border	150bp: GTACGTGCCCAGCTATCTCC 500bp: GGACCAAGATGAGAGAGCGG	CGAAAACACCTGCAATCCTGGGGCAGTACTAGAACTAGCC CAGGTCCACCTGCCGACAGCATTCTTTTTTTAGTCGTAAA
3' border	150bp: CTCCATCCCATGCGCAAATG 500bp: CGGTTGATGACGGACTGACA	AGGCATCACCTGCTCGGTCGACCTAGTTCTCAGAAATGTA TGGATCCACCTGCAGTAATGCGAGCTAACATTGCTCTCAG
Gene	N/A	AATACCCACCTGCGAGATGCTCTAGAGGGTAGCAAACGGT GACAAACACCTGCTAGTTCGAGCTGTCTGGTCTTCTACAC
Screening/ sequencing	Fwd: CCATTCGCCTCGTCACTGAT Rev: GATTCCGGTGTGTGTCCCAT	Fwd: GGTGGTTGTTTTCGCCTGAC Rev: TGGTGGAGCAAGCAAGAGAG

Chemistry of *perA* transformants

Successful *perA* repairs were inoculated into Reason, a perennial ryegrass cultivar following the methods of Miller et al. (2022). Dahurelmusin A (DA), produced by AR48, was used as a control to confirm that other secondary metabolite pathways had not been affected by the insertion. Sub-samples of the ground plant material (25 mg ± 5 mg) were extracted for 1 hour by end-over-end rotation with 1 mL of 50% methanol containing homoperamine (0.85 µg/mL) as an internal standard. Extracts were centrifuged (4000 g, 5 min) and filtered (13 mm 0.45 µm PFTE syringe filter) into 2 mL amber HPLC vials for analysis. Peramine, DA and homoperamine were detected using a LCMS-2020 (Shimadzu Corporation, Kyoto, Japan). Compounds were chromatographically separated using a Synergi Polar-RP column (100 × 2.1 mm, 2.5 µm; Phenomenex, USA) at a flow rate of 400 µL/min with the following gradient of 0.1% aqueous formic acid (A) and 95% acetonitrile (0.1% formic acid) (B); initially at 5% B, held for 2 min, then linear gradient to 55% B at 12 min, followed by linear gradient to 90% B at 12.5 min, held for 2 min, then returned to initial conditions at 15.5 min before equilibrating for 3.5 min prior to subsequent injections. Detection was via electrospray ionisation with the compounds detected and quantified by their $[M+H]^+$ ions; peramine (248 *m/z*) 5.45 min, homoperamine (262 *m/z*) 6.36 min, and DA (355 *m/z*) 9.38 min.

Results

CRISPR-Cas9 assisted *perA* gene repair in AR48

Insertion of the missing 236 bp into the condensation domain of the NRPS encoding *perA* gene in AR48 using CRISPR-Cas9 was investigated (Figure 1). Two guides located across the insertion site were used, guide 434 (forward strand) and guide 912 (reverse strand). For each guide, DNA templates with two different borders were transformed, approximately 150 bp either side (Figure 1a) and approximately 500 bp either side (Figure 1b). Sequencing of approximately 1 kb was done across the insertion site (Figure 2),

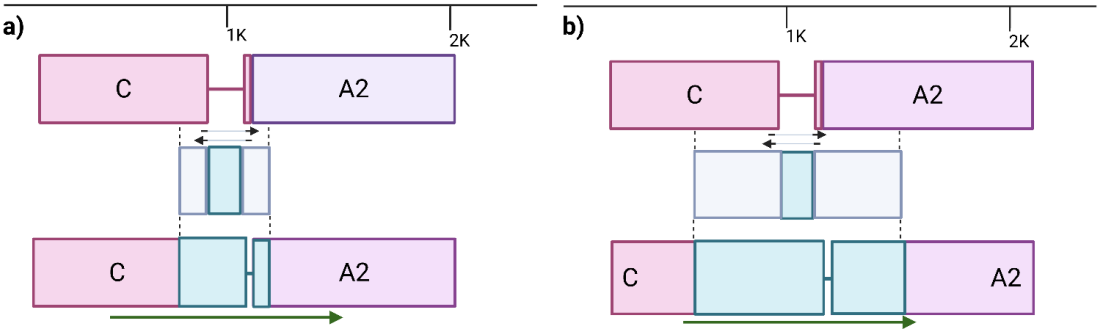

Figure 1 Schematic diagram of the CRISPR-Cas9 assisted AR48 *perA* gene repair methodology. The guide 434 (forward strand) and guide 912 (reverse strand) are represented by the black arrows that sits either side of the insertion site with the grey line indicating absence of sequence. Green arrow is region sequenced. The two templates used are a) approximately 150 bp borders and b) approximately 500 bp borders. The colours: pink/purple (AR48 sequence), and blue (AR1 sequence - light blue indicating border region). Created in BioRender. Miller, T. (2025) https://BioRender.com/8apvnor.

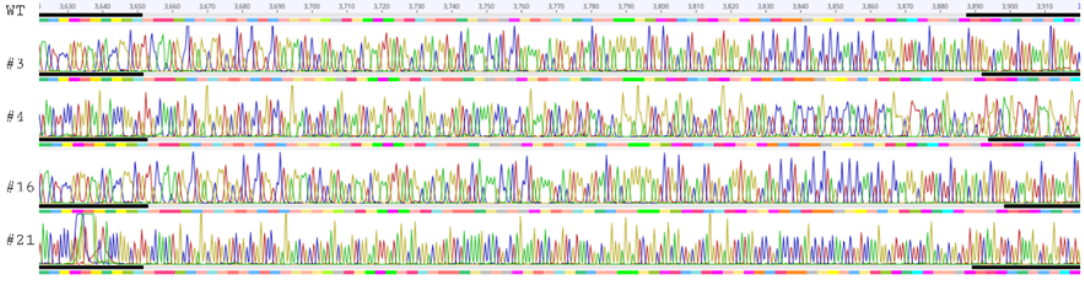

Figure 2 Sequencing results of CRISPR-Cas9 assisted AR48 *perA* gene repair. Sequencing alignment of chromatographs from a single primer for AR48 wild-type (WT) and AR48 *perA* gene repaired transformants (#3, #4, #16, and #21). Each transformant has a chromatograph line (nucleotide coloured), DNA sequence line (black same nucleotide and grey missing nucleotide), and amino acids translation line (coloured by amino acids).Created in BioRender. Miller, T. (2025) https://BioRender.com/spcxw85.

Table 3 Chemistry of the CRISPR-Cas9 assisted repair of AR48 *perA*.

	FL1 WT	S.E	AR48 WT	S.E	AR48 g912 #3	S.E	AR48 g912 #4	S.E	AR48 g912 #16	S.E	AR48 g912 #21	S.E
n	2		3		3		3		3		3	
Peramine (mg/kg)	63.5	6.7	0	0	0	0	0	0	0	0	0	0
DA (mg/kg)	0	0	15.8	2.7	17.9	2.0	12.1	5.9	11.5	0.3	45.6	14.0

DA = Dahurelmusin A, # = independent transformants, S.E = standard error of the mean.

spanning from approximately 450 bp outside (Figure 1a) or approximately 100 bp outside (Figure 1b) of each border.

There were no insertions for guide 434, despite 75 transformants in total being screened from both template border types. Guide 912 had 1/18 (5.5%) targeted insertions for the 150 bp border (#21) and 3/18 (17%) targeted insertions for the 500 bp border (#3, #4, and #16) (Table 3). Chemical analysis undertaken on perennial ryegrass plants infected with either transformants #3, #4, #16, and #21 showed no production of peramine, however the control compound DA was detected for all samples. To note, #21 DA levels were elevated in comparison to all other protoplast derived samples but were within normal range (Table 3).

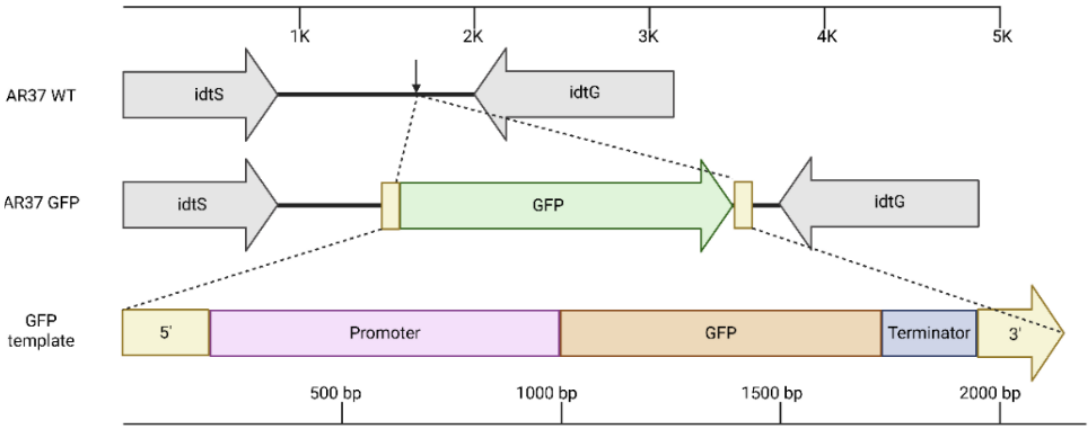

Figure 3 Schematic diagram of the CRISPR-Cas9 assisted AR37 GFP gene insertion. The reporter gene *gfp* expressed under the constitutive Tef (Translation Elongation Factor 1-alpha from Aureobasidium) promoter and Tgla (glucoamylase from *Aspergillus* species) terminator was inserted between *idtS* and *idtG* (indole diterpene secondary metabolite genes) using CRISPR-Cas9 in AR37. The location and direction of the gene is indicated by the coloured arrows, with guide TM07 as the small vertical arrow. Guide TM07 was used to create a double stranded DNA break by the CRISPR-Cas9 machinery at the targeted location triggering cell mediated homologous repair using the template provided which contained a functional *gfp* gene. The top scale refers to AR37 WT and AR37 GFP diagram while the bottom scale refers to GFP template diagram. Created in BioRender. Miller, T. (2025) https://BioRender.com/hluj0us.

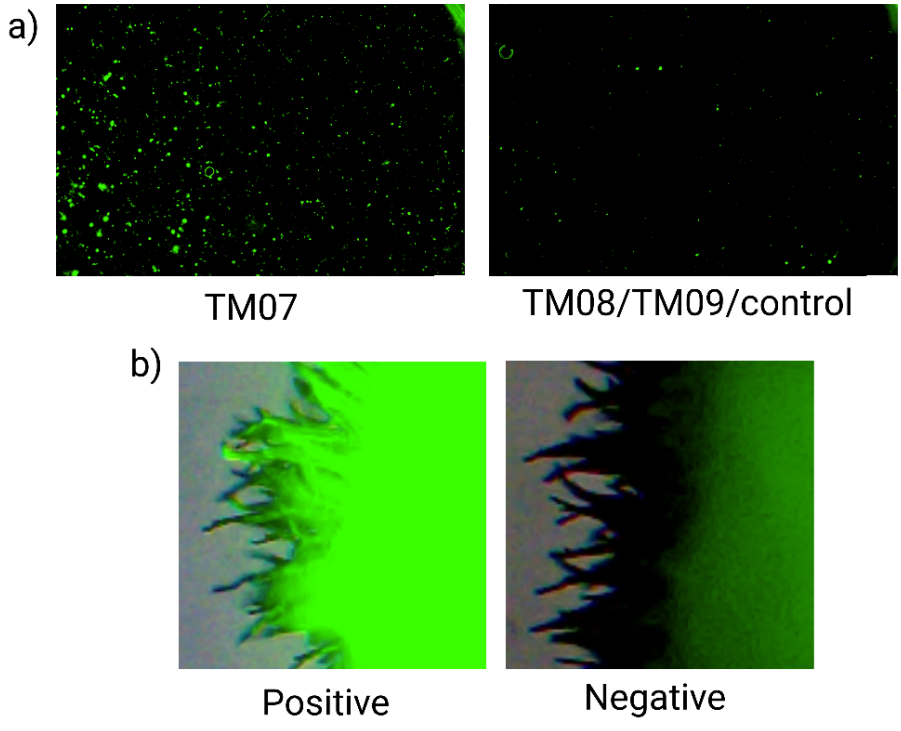

Figure 4 Microscopy images of CRISPR-Cas9 assisted *gfp* gene insertion transformants. a) Whole plate stitched image of regenerative media FL1 transformant plate using a *gfp* channel comparing different guides (TM07/TM08/TM09) and control (water). b) Single AR37 transformant sub-cultured from TM07 transformation plate into potato dextrous plate imaged used *gfp* channel. Positive for fluorescence or negative for fluorescence. Created in BioRender. Miller, T. (2025) https://BioRender.com/g91ihae.

Table 4 Screening of AR37 CRISPR-Cas9 assisted *gfp* gene insertion.

Transformant	Fluorescent	PCR	qPCR	Sequencing	Ectopic	IdtS	IdtG
AR37 #8	Yes	GFP	4	L-GFP-R	Yes	Yes	Yes
AR37 #30	Yes	GFP	5	L-L-GFP-R-R	Yes	Yes	Yes
AR37 #31	Yes	GFP	5	L-GFP-R-R	Yes	Yes	Yes
AR37 #39	Yes	GFP	3	L-L-GFP-R	Yes	Yes	Yes
AR37 #43	Yes	GFP	2	L-L-GFP-R-R	Yes	Yes	Yes
AR37 #61	Yes	WT	1	L-R	Yes	Yes	Yes
AR37 #114	Yes	GFP	1	L-GFP-R	No	Yes	Yes
AR37 #174	Yes	WT	1	L-R	Yes	Yes	Yes

L= 5' border, R= 3' border, WT= wild type size, GFP= gene / PCR size.

CRISPR-Cas9 assisted *gfp* insertion into the indole diterpene pathway in AR37

Insertion of the reporter gene *gfp* (724 bp) into the IDT pathway between genes *idtS* and *idtG* was investigated in the *Epichloë* strains Fl1 and AR37 (Figure 3). Three guides TM07 (forward strand), TM08 (reverse strand) and TM09 (reverse strand) all within 140 bp of each other were transformed into Fl1 protoplast with a *gfp* construct which used 200 bp borders (Figure 3). Whole plate image stitching was used to visually assess the success of the transformation (Figure 4a). The best guide was then transformed into AR37 protoplast and further analysed for gene insertion events (Figure 4b).

Microscopy screening of AR37 sub-cultured transformants identified that 8/18 (44%) fluoresced. Genetic screening identified that 6/8 (75%) of these had the *gfp* gene inserted into the target locus, with *idtS* and *idtG* genes retained for all six transformants, and of those transformants only transformant #114 (17%) contained no ectopic integrations. This single transformant also did not have any border duplications at either one or both ends. The absence of border duplication at both ends was only seen for one other transformant but this transformant #8 had an additional 3 ectopic copies. The other five remaining targeted insertions had some form of border duplications as well as ectopics (Table 4).

Discussion

CRISPR-Cas9 assisted *perA* gene repair in AR48

For the first time, targeted gene insertion was achieved within genetically intractable *Epichloë* species using CRISPR. This was attained through CRISPR-Cas9 insertion of 236 bp into the condensation domain of the *perA* gene in AR48. Four successful transformants were identified for guide 912 across both border sizes, with three using the larger border, while guide 434 had no successful transformants. Guide design is therefore the most important aspect followed by border size.

For *Epichloë* spp. using traditional HR the border homology arms are between 500 bp and 1000 bp (Johnson et al. 2021). For CRISPR assisted HR the insertion size dictates the border homology arms. For insertions below 200 bp homology arms 30 bp to 50 bp are required and a linear single stranded DNA template is recommended. In contrast, for insertions more than 200 bp homology arms 500 bp to 1000 bp are required and a linear double stranded DNA template is recommended (Patrick et al. 2015). For this experiment, a linear double stranded DNA with the longer arm of 500 bp, rather than the shorter arm of 150 bp, was more successful which agrees with these generalised guidelines.

When all four of the above successful transformants were inoculated into grass seedlings, no peramine was detected in the subsequent infected plants. However, the control DA compound was present and therefore these transformants were actively expressing secondary metabolites and the chemistry analysis method was robust. DA was used as a control because it was extracted alongside and analysed with peramine. Further investigation of the gene repair in terms of mRNA and/or the associated NRPS expression levels is required to understand the absence of peramine in these strains, although it is possible that other SNPs within the AR48 *perA* gene could be rendering it non-functional.

All transformants were derived from the same protoplast batch and inoculated into the same seed line. Transformant #21 had the highest DA levels for all three analysed plants (27-73 ppm) compared to the other transformants and protoplast derived WT (7-24 ppm). However, these levels are within the range typically seen for AR48. The AR48 *perA* repair is an example of a CRISPR-Cas9 targeted insertion within an exon. This is potentially one of a handful of these

types of genetic modifications, the only other being in a mushroom (Eom et al. 2025). CRISPR-Cas9 gene repair through insertion is more common in humans to restore genes which cause disease; however, the insertions are commonly only a few base pairs (Xu et al. 2017; Yang et al. 2023) and larger insertions are accomplished by cutting using the guide in the intron and replacing whole exons (Pickar-Oliver et al. 2021). This could not be achieved for *perA* as there are no introns. One challenge encountered for targeted insertion within a gene is that the guide needs to be removed to prevent unwanted CRISPR-Cas9 editing events *e.g.,* NHEJ events that could create SNPs or indels. A further challenge encountered is the repair needs to be perfect to prevent changes to the gene sequence. These two challenges are not encountered when inserting DNA in non-coding regions *e.g., gfp* insertion into AR37.

CRISRP-Cas9 assisted *gfp* insertion into the indole diterpene pathway in AR37

For the initial investigation into CRISPR-Cas9 whole gene insertion into genetically intractable *Epichloë* strains *e.g.,* AR37, the reporter gene *gfp* was chosen. This was because successful integration along with expression could be easily assessed using fluorescent microscopy imaging of transformants. This screening stage is typically tedious when working with bioactive secondary metabolites as the gene is typically only expressed at sufficient levels *in planta*. All transformants therefore must be genetically screened and inoculated into seedlings before chemistry can be undertaken to determine functional gene insertions (Johnson et al. 2021).

Landing pads are sites either identified or inserted into genomes that assist in future gene editing. These sites are identified as being genetically stable and can contain selectable markers, recombinase sites, or promoters. These landing pads have not been identified in *Epichloë* spp. and therefore a process was required to select the location of *gfp* gene insertion for successful expression. All future gene insertions would need to be expressed *in planta* and therefore the known IDT secondary metabolite pathway, present in most marketed *Epichloë* strains, was selected. Within the pathway, the intergenic region between *idtS* and *idtG* was chosen as this is part of the core cluster for IDT expression, rather than accessory genes which may not be present in all strains of interest. In addition, this is where two terminators are present therefore reducing the likelihood of disrupting gene expression of surrounding genes, which might occur if the insertion was close to undefined promoter regions. *In planta* chemistry still needs to be done on these successful insertions to investigate IDT production to test this hypothesis.

Guide TM07 was the only guide that had visually more fluorescent colonies on whole plate images than the control. This could indicate the presence of CRISPR-Cas9 assisted targeted gene insertion events alongside the traditional homologous targeted or ectopic insertion events which occurred at a much lower frequency in the control. Again, the guide selection was important for successful CRISPR-Cas9 targeted insertion. To note, the location chosen is an *in planta* expressed secondary metabolite cluster, and the inserted *gfp* was expressed in culture. This is contradictory to previous evidence that shows this region as heterochromatin in culture which is indicative of gene repression (Chujo & Scott 2014). This cluster therefore might be regulated further by additional means such as transcription factors, which would not affect *gfp* expression as it is expressed constitutively.

For the first time successful CRISPR-Cas9 targeted gene insertion was achieved in AR37 through the insertion of the *gfp* gene (1.7-2.1 kb depending on insertion mechanism) into the intergenic region between the IDT genes *idtS* and *idtG*. Just under half of the transformants fluoresced (44%) when assessed by fluorescent microscopy. The border size was reduced to keep the overall template size manageable for PCR amplification, and though smaller than the recommended size for the insertion size *i.e.* at least 500 bp border for a 2 kb insert (Patrick et al. 2015), the success rate was relatively high.

The majority of the AR37 fluorescent transformants did have additional multiple ectopic gene insertions. Random integration of genes into commercial *Epichloë* strains has been previously achieved (Hettiarachchige et al. 2019) and therefore this was not unexpected. Optimising the template concentration might reduce these ectopic events however this could also reduce targeted integration events, therefore an equilibrium would need to be achieved.

CRISPR-Cas9 gene editing is known to have unintended events occur at the target locus such as chromosomal loss (Hunt et al. 2023; Park et al. 2023). Given this locus is sub-telomeric, *gfp* targeted gene inserted transformants were checked for the presence of *idtS* and *idtG*. All transformants contained both genes suggesting retention of the telomere. Further investigation into other unintended events could be undertaken using genome sequencing *e.g.,* foot-printless through confirmation of loss of the CRISPR-Cas9 plasmid containing the guide and enzymatic machinery sequence.

When the *gfp* gene was inserted into the target

location, border duplication at one or both ends occurred in the majority of the AR37 transformants, or a 50% border duplication rate if each border was assessed individually. This indicates that in AR37, double stranded DNA breaks can be equally repaired by HR or NHEJ, this is termed asymmetrical repair *i.e.,* one end is resected inducing HR therefore no border duplication, and the other end has minimal resection or blocked resection inducing NHEJ therefore border duplication (Xue & Greene 2021). This has been reported in *Aspergillus niger*, where a CRISPR-Cas9 insertion resulted in 91.4% insertion rate but with 20.3% of those being HR at the 5' end and NHEJ at the 3' end (Fritsche et al. 2024).

Conclusions

For the first time targeted DNA insertion was achieved in genetically intractable *Epichloë* species using CRISPR-Cas9. A 236 bp DNA fragment was inserted into the exonic region of the condensation domain of the *perA* gene in AR48. However, no peramine was detected prompting future analysis into potential reasons. In addition, the gene *gfp* was successfully inserted into the intergenic region of the IDT cluster in AR37. Both these experiments provide vital information on CRISPR-Cas9 insertion parameters for *Epichloë* spp.

ACKNOWLEDGEMENTS

We thank Concordia University for providing the CRISR-Cas9 plasmid delivery system ANEp8_Cas9_LIC plasmid (Song et al. 2018), Jaspreet Singh for contacting Concordia University and acquiring their CRISPR technology and Anouck de Bonth for the immunoblotting to detect endophyte *in planta.*

REFERENCES

Berry D, Takach JE, Schardl CL, Charlton ND, Scott B, Young CA. 2015. Disparate independent genetic events disrupt the secondary metabolism gene *perA* in certain symbiotic *Epichloë* species. *Applied and Environmental Microbiology* 81: 2797–2807. https://doi.org/10.1128/AEM.03721-14

Caradus JR, Johnson LJ. 2019. Improved adaptation of temperate grasses through mutualism with fungal endophytes. *In Endophyte Biotechnology: Potential for Agriculture and Pharmacology*, pp. 85–108. CABI. https://doi.org/10.1079/9781786399427.0085

Chu VT, Weber T, Graf R, Sommermann T, Petsch K, Sack U, Volchkov P, Rajewsky K, Kühn R. 2016. Efficient generation of Rosa26 knock-in mice using CRISPR/Cas9 in C57BL/6 zygotes. *BMC Biotechnology* 16: 4. https://doi.org/10.1186/s12896-016-0234-4

Chujo T, Scott B. 2014. Histone H3K9 and H3K27 methylation regulates fungal alkaloid biosynthesis in a fungal endophyte–plant symbiosis. *Molecular Microbiology* 92: 413–434. https://doi.org/10.1111/mmi.12567

Eom H, Choi Y-J, Nandre R, Kim M, Oh Y-L, Kim S, Nakazawa T, Honda Y, Ro H-S. 2025. Targeted insertion of heterogeneous DNA using Cas9-gRNA ribonucleoprotein-mediated gene editing in *Ganoderma lucidum*. *Bioengineered* 16: 2458376. https://doi.org/10.1080/21655979.2025.2458376

Florea S, Jaromczyk J, Schardl CL. 2021. Non-transgenic CRISPR-Mediated knockout of entire ergot alkaloid gene clusters in slow-growing asexual polyploid fungi. *Toxins* 13: 153. https://doi.org/10.3390/toxins13020153

Fritsche S, Reinfurt A, Fronek F, Steiger MG. 2024. NHEJ and HDR can occur simultaneously during gene integration into the genome of *Aspergillus niger*. *Fungal Biology and Biotechnology* 11: 10. https://doi.org/10.1186/s40694-024-00180-7

Hendriks D, Clevers H, Artegiani B. 2020. CRISPR-Cas tools and their application in genetic engineering of human stem cells and organoids. *Cell Stem Cell* 27: 705–731. https://doi.org/10.1016/j.stem.2020.10.014

Hettiarachchige IK, Elkins AC, Reddy P, Mann RC, Guthridge KM, Sawbridge TI, Forster JW, Spangenberg GC. 2019. Genetic modification of asexual *Epichloë* endophytes with the *perA* gene for peramine biosynthesis. *Molecular Genetics and Genomics* 294: 315–328. https://doi.org/10.1007/s00438-018-1510-x

Hunt JMT, Samson CA, Rand AD, Sheppard HM. 2023. Unintended CRISPR-Cas9 editing outcomes: a review of the detection and prevalence of structural variants generated by gene-editing in human cells. *Human Genetics* 142: 705–720. https://doi.org/10.1007/s00439-023-02561-1

Jiang C, Lv G, Tu Y, Cheng X, Duan Y, Zeng B, He B. 2021. Applications of CRISPR/Cas9 in the synthesis of secondary metabolites in filamentous fungi. *Frontiers in Microbiology* 12: 164. https://doi.org/10.3389/fmicb.2021.638096

Johnson LJ, de Bonth AC, Briggs LR, Caradus JR, Finch SC, Fleetwood DJ, Fletcher LR, Hume DE, Johnson RD, Popay AJ. 2013. The exploitation of *Epichloë* endophytes for agricultural benefit. *Fungal Diversity* 60: 171–188. https://doi.org/10.1007/s13225-013-0239-4

Johnson LJ, Caradus JR. 2019. The science required to deliver *Epichloë* endophytes to commerce. *In Endophytes for a Growing World*, pp. 343. (Elsevier). https://doi.org/ https://doi.

org/10.1017/9781108607667

Johnson LJ, Bastías DA, Caradus JR, Chettri P, Forester NT, Mace WJ, Miller TA, Moon CD, Voisey CR, Zhang W. 2021. The dynamic mechanisms underpinning symbiotic *Epichloë*–grass interactions: Implications for sustainable and resilient agriculture. *In Microbiome Stimulants for Crops*, pp. 73–108. (Elsevier). DOI: https://doi.org/10.1016/C2019-0-04354-3

Kato T, Hara S, Goto Y, Ogawa Y, Okayasu H, Kubota S, Tamano M, Terao M, Takada S. 2017. Creation of mutant mice with megabase-sized deletions containing custom-designed breakpoints by means of the CRISPR/Cas9 system. *Scientific Reports* 7: 59. https://doi.org/10.1038/s41598-017-00140-9

Liu Z, Dong H, Cui Y, Cong L, Zhang D. 2020. Application of different types of CRISPR/Cas-based systems in bacteria. *Microbial Cell Factories* 19: 1-14. https://doi.org/10.1186/s12934-020-01431-z

Menchaca A, Dos Santos-Neto P, Mulet A, Crispo M. 2020. CRISPR in livestock: From editing to printing. *Theriogenology* 150: 247–254. https://doi.org/10.1016/j.theriogenology.2020.01.063

Miller TA. 2018. Insect bioactive capabilities of *Epichloë festucae* var. *lolii* AR48 infected *Lolium perenne*: a thesis presented in partial fulfilment of the requirements for the degree of Doctor of Philosophy in Biochemistry at Massey University, Manawatū, New Zealand. *Unpublished thesis, Massey University*. http://hdl.handle.net/10179/15178

Miller TA, Hudson DA, Johnson RD, Singh JS, Mace WJ, Forester NT, Maclean PH, Voisey CR, Johnson LJ. 2022. Dissection of the epoxyjanthitrem pathway in *Epichloë* sp. Lp TG-3 strain AR37 by CRISPR gene editing. *Frontiers in Fungal Biology* 3: 944234. https://doi.org/10.3389/ffunb.2022.944234

Moradpour M, Abdulah SNA. 2020. CRISPR/dCas9 platforms in plants: strategies and applications beyond genome editing. *Plant Biotechnology Journal* 18: 32–44. https://doi.org/10.1111/pbi.13232

Panaccione DG, Johnson RD, Wang J, Young CA, Damrongkool P, Scott B, Schardl CL. 2001. Elimination of ergovaline from a grass–*Neotyphodium* endophyte symbiosis by genetic modification of the endophyte. *Proceedings of the National Academy of Sciences of the United States of America* 98: 12820–12825. https://doi.org/10.1073/pnas.221198698

Park SH, Cao M, Bao G. 2023. Detection and quantification of unintended large on-target gene modifications due to CRISPR/Cas9 editing. *Current Opinion in Biomedical Engineering* 28: 100478. https://doi.org/10.1016/j.cobme.2023.100478

Patrick M, Gearing M, Mork C, Stroik S. 2015. CRISPR 101: Homology Directed Repair. 2025. https://doi.org/10.1016/j.cobme.2023.100478 Pickar-Oliver A, Gough V, Bohning JD, Liu S, Robinson-Hamm JN, Daniels H, Majoros WH, Devlin G, Asokan A, Gersbach CA. 2021. Full-length dystrophin restoration via targeted exon integration by AAV-CRISPR in a humanized mouse model of Duchenne muscular dystrophy. *Molecular Therapy* 29: 3243–3257. https://doi.org/10.1016/j.ymthe.2021.09.003

Pickar-Oliver A, Gough V, Bohning JD, Liu S, Robinson-Hamm JN, Daniels H, Majoros WH, Devlin G, Asokan A, Gersbach CA. 2021. Full-length dystrophin restoration via targeted exon integration by AAV-CRISPR in a humanized mouse model of Duchenne muscular dystrophy. Molecular Therapy 29: 3243–3257. https://doi.org/10.1016/j.ymthe.2021.09.003

Rowan DD, Dymock JJ, Brimble MA. 1990. Effect of fungal metabolite peramine and analogs on feeding and development of Argentine stem weevil (*Listronotus bonariensis*). *Journal of Chemical Ecology* 16: 1683–1695. https://doi.org/10.1007/BF01014100

Schardl CL. 1996. *Epichloë* species: fungal symbionts of grasses. *Annual Review of Phytopathology* 34: 109–130. https://doi.org/10.1146/annurev.phyto.34.1.109

Schardl CL, Young CA, Hesse U, Amyotte SG, Andreeva K, Calie PJ, Fleetwood DJ, Haws DC, Moore N, Oeser B. 2013. Plant-symbiotic fungi as chemical engineers: multi-genome analysis of the *Clavicipitaceae* reveals dynamics of alkaloid loci. *PLOS Genetics* 9: e1003323. https://doi.org/10.1371/journal.pgen.1003323

Song L, Ouedraogo J-P, Kolbusz M, Nguyen TTM, Tsang A. 2018. Efficient genome editing using tRNA promoter-driven CRISPR/Cas9 gRNA in *Aspergillus niger*. *PLOS ONE* 13: e0202868. https://doi.org/10.1371/journal.pone.0202868

Spiering MJ, Moon CD, Wilkinson HH, Schardl CL. 2005. Gene clusters for insecticidal loline alkaloids in the grass-endophytic fungus *Neotyphodium uncinatum*. *Genetics* 169: 1403-1414. https://doi.org/10.1534/genetics.104.035972

Tanaka A, Tapper BA, Popay A, Parker EJ, Scott B. 2005. A symbiosis expressed non-ribosomal peptide synthetase from a mutualistic fungal endophyte of perennial ryegrass confers protection to the symbiotum from insect herbivory. *Molecular Microbiology* 57: 1036-1050. https://doi.org/10.1111/j.1365-2958.2005.04747.x

Tong XL, Fang CY, Gai TT, Shi J, Lu C, Dai FY. 2018.

Applications of the CRISPR/Cas9 system in insects. *Hereditas (Yi Chuan)* 40: 266–278. https://doi.org/10.16288/j.yczz.17-263

Uyhazi KE, Bennett J. 2021. A CRISPR view of the 2020 Nobel Prize in Chemistry. *The Journal of Clinical Investigation* 131. https://doi.org/10.1172/JCI145214

Wang R, Clarke BB, Belanger FC. 2018. CRISPR-Cas9 gene knockout of the *Epichloë festucae* antifungal protein gene. *Microorganisms* 9(1): 140. https://doi.org/10.3390/microorganisms9010140

Xu Q, Hou Y-x, Chang X-b. 2017. CRISPR/Cas9-mediated three nucleotide insertion corrects a deletion mutation in MRP1/ABCC1 and restores its proper folding and function. *Molecular Therapy – Nucleic Acids* 7: 429-438. https://doi.org/10.1016/j.omtn.2017.05.005

Xue C, Greene EC. 2021. DNA repair pathway choices in CRISPR-Cas9-mediated genome editing. *Trends in Genetics* 37: 639-656. https://doi.org/10.1016/j.tig.2021.02.008

Yang F, Wang Y, Wang Q, Pang J, Liu G, Yang Y, Qin S, Zhang Y, Lai Y, Fu B. 2023. Efficient repair of human genetic defect by CRISPR/Cas9-mediated interlocus gene conversion. *Life Medicine* 2: lnad042. https://doi.org/10.1093/lifemedi/lnad042

Young CA, Tapper BA, May K, Moon CD, Schardl CL, Scott B. 2009. Indole-diterpene biosynthetic capability of *Epichloë* endophytes as predicted by ltm gene analysis. *Applied and Environmental Microbiology* 75: 2200-2211. https://doi.org/10.1128/AEM.00953-08

Zhang L, Jia R, Palange NJ, Satheka AC, Togo J, An Y, Humphrey M, Ban L, Ji Y, Jin H. 2015. Large genomic fragment deletions and insertions in mouse using CRISPR/Cas9. *PLOS ONE* 10: e0120396. https://doi.org/10.1371/journal.pone.012039